

# ROLE OF RADIOFREQUENCY POWER ON THE CRYSTALLOGRAPHIC, MORPHOLOGICAL AND OPTICAL PROPERTIES OF SPUTTERED ALUMINUM THIN FILMS

PAPEL DE LA POTENCIA DE LA RADIOFRECUENCIA EN LAS PROPIEDADES CRISTALOGRÁFICAS, MORFOLÓGICAS Y ÓPTICAS DE LAS CAPAS DELGADAS DE ALUMINIO DEPOSITADAS MEDIANTE «SPUTTERING »

R. RAMOS-BLAZQUEZ<sup>a</sup>, F. SOLIS-POMAR<sup>a†</sup>, A. FUNDORA-CRUZ<sup>b</sup>, A. COLLADO-HERNANDEZ<sup>a</sup>, C. GARCIA-RODRIGUEZ<sup>a</sup>, M.J. MARTÍNEZ-CARREÓN<sup>a</sup>, A. FRAGIEL<sup>c</sup>, A. MARTINEZ-HUERTA<sup>a</sup> AND E. PEREZ-TIJERINA<sup>a</sup>

a) Centro de Investigación en Ciencias Físico Matemáticas, Facultad de Ciencias Físico Matemáticas, Universidad Autónoma de Nuevo León, 66451 Nuevo León, México; francisco.solispm@uanl.edu.mx <sup>†</sup>

b) Instituto Superior de Tecnologías y Ciencias Aplicadas (InSTeC), Universidad de La Habana, 10400 La Habana, Cuba

c) Laboratorio de Física Aplicada, Modelos Fundamentales, Fluidos y Plasmas, Centro de Física, Instituto Venezolano de Investigaciones Científicas (IVIC), 1020-A Caracas, Venezuela.

<sup>†</sup> corresponding author

Recibido 22/9/2025; Aceptado 20/11/2025

Aluminum (Al) thin films are of great interest for applications in telecommunications, microelectronics, and the automotive industry, among others, due to their high conductivity, excellent optical properties and low weight. Their properties depend on the deposition technique and its parameters. In this work, the crystallographic, morphological, and optical characteristics of Al thin films grown by radio-frequency (RF) magnetron sputtering were analyzed. An aluminum target was used in an argon (Ar) atmosphere, and the effect of sputtering power on film properties was investigated. The samples were characterized by X-ray diffraction (XRD), Scanning Electron Microscopy (SEM), Atomic Force Microscopy (AFM), and UV-Vis Spectroscopy. The crystalline quality improved with increasing power. AFM and SEM results revealed an increase in roughness, thickness, and grain size with higher sputtering power. UV-Vis spectroscopy showed lower diffuse reflectance at lower power across the 190-900 nm range. The enhancement of film properties is mostly attributed to the increased kinetic energy of sputtered species, directly related to the applied RF power.

Las películas delgadas de aluminio (Al) son de gran interés para aplicaciones en telecomunicaciones, microelectrónica y la industria automotriz, entre otras, debido a su alta conductividad, excelentes propiedades ópticas y bajo peso. Sus propiedades dependen de la técnica de depósito y sus parámetros. En este trabajo, se analizaron las características cristalográficas, morfológicas y ópticas de películas delgadas de Al crecidas mediante pulverización catódica (sputtering) magnetrón de radiofrecuencia (RF). Se utilizó un blanco de aluminio en una atmósfera de argón (Ar), y se investigó el efecto de la potencia de pulverización en las propiedades de la película. Las muestras se caracterizaron por Difracción de Rayos X (XRD), Microscopía Electrónica de Barrido (SEM), Microscopía de Fuerza Atómica (AFM) y Espectroscopía UV-Vis. La calidad cristalina mejoró al aumentar la potencia. Los resultados de AFM y SEM revelaron un aumento en la rugosidad, el espesor y el tamaño de grano con una mayor potencia de pulverización. La espectroscopía UV-Vis mostró una menor reflectancia difusa a menor potencia en el rango de 190-900 nm. La mejora de las propiedades de la película se atribuye principalmente al aumento de la energía cinética de las especies pulverizadas, directamente relacionada con la potencia de RF aplicada.

Keywords: Aluminum (Aluminio), Thin films (Capas delgadas), magnetron sputtering (*sputtering* con magnetrón), Radio Frequency power (Potencia de radiofrecuencia)

## I. INTRODUCTION

Aluminum (Al) thin films are employed in various technological fields, including telecommunications, microelectronics, optics, and the automotive industry, among others, due to their high conductivity, reflectance, and corrosion resistance [1]. These properties, combined with the advantage of being lightweight, make their study particularly relevant. The structural characteristics of thin films are strongly influenced by the synthesis method used. According to the literature, physical methods such as thermal and vapor deposition are the most commonly employed [1].

film synthesis that involves the erosion of material from the surface of a bulk material, known as target, by means of the bombardment with accelerated ions. This method is highly advantageous, as it produces uniform thin films with excellent reproducibility and is scalable to large industrial facilities. The final properties of the films are determined by the conditions used during the deposition process. In the case of magnetron sputtering, factors such as applied power [2-4], deposition time [5, 6], working pressure, the type of the gases used [7, 8], substrate temperature [9-11], and target-to-substrate distance [12], among others, play a crucial role in defining their characteristics.

Magnetron sputtering is a widely used technique for thin In the context of magnetron sputtered Al thin films, an

increment of the hardness for the coatings deposited at 200 sccm from 0.62 to 1.31 GPa has been reported, as power increased from 500 to 2000 W, and an increase in the deposition rate was detected as the Ar flow rate raised from 200 to 500 sccm [13]. Moreover, Al thin films grown on steel substrates presented enhanced crystallinity and a decrease in root-mean-squared roughness values as higher substrate temperatures were employed in the synthesis procedure [14]. Abid Iqbal et al. [3] reported that an increase of sputtering power enhances the kinetic energy of ions, resulting in the production of highly c-axis oriented aluminum nitride thin films. However, they also noted how excessively high power can negatively affect the crystal structure due to the elevated kinetic energy of secondary atoms.

Although significant progress has been made in developing Al thin films synthesized by magnetron sputtering, a comprehensive understanding of how the deposition parameters influence the resulting functional characteristics is crucial. Aluminum thin films have a broad range of technological applications, such as reflective the coating for telescopes [15], antibacterial surfaces [16], and protective or decorative coatings [1], where precise control over crystallographic, morphological, and optical behavior is required, since each application demands specific and distinct film properties. Therefore, establishing clear correlations between sputtering conditions and the resulting film features is essential to optimize their performance for specific applications. In this context, the present study systematically investigates the effect of RF sputtering power on the crystallographic, morphologic and optical properties of Al thin films. The work provides a quantitative statistical analysis of grain size distributions, reports diffuse optical reflectance behaviour and offers a fully reproducible set of deposition parameters with detailed explanations of each observed trend.

## II. METHODOLOGY

### II.1. Thin films synthesis.

Al thin films were synthesized on clean BK7 glass substrates (25 mm × 25 mm) by RF magnetron sputtering using a UHV Standard Spherical Chamber from Kurt J. Lesker, with no intentional heating applied to the samples. Before deposition, the substrates were pre-sputtered for 40 minutes to ensure surface cleanliness. The deposition procedure consisted of employing an Al target (2" diameter, 1/4" thickness, 99.99% purity) from Advanced Engineering Materials and a radio-frequency (RF) power source operating at 13.56 MHz, with variable power output. The Al target was mounted on the cathode over the magnetron head and the glass substrates were placed on the anode holder at a fixed distance of 9 cm. The chamber was evacuated using mechanical and turbomolecular pumps until a base pressure of  $3.5 \times 10^{-5}$  Torr was reached. Subsequently, Ar gas (99.999% purity) was introduced at a flow rate of 40 sccm, until a working pressure of 5.0 mTorr was achieved. After stabilization of the working pressure in the chamber, the RF power source was activated. The RF power was varied from 120-180 W to

study its effect on the film properties, while the deposition time was fixed at 15 minutes. Lower powers were avoided because they produce thinner films with reduced crystallinity and a stronger dependence of surface morphology on the substrate [17]. On the other hand, higher powers may lead to re-sputtering effects [18].

Table 1. Deposition conditions for the Al thin films.

Parameter	Value
RF-power (W)	120, 140, 180
Working pressure (mTorr)	5.0
Ar flux (sccm)	40
Deposition time (min)	15
Target-Substrate distance (cm)	9

### II.2. Characterization.

The crystalline structure of the films was studied by X-Ray diffraction using an X'Pert3 Powder diffractometer from Malvern Panalytical, operating with a Cu K source ( $\lambda = 1.5406 \text{ \AA}$ ) at 45 kV and 40 mA. Diffraction patterns were processed using the X'Pert Highscore Plus software and indexed with the International Centre for Diffraction Data (ICDD) database. Film morphology was examined by field-emission scanning electron microscopy (FESEM) and atomic force microscopy (AFM). FESEM images and EDS spectra were measured using the Nova NanoSEM 200 microscope from FEI, while AFM images were obtained using the NX10 atomic force microscope from Park Systems, operating in non-contact mode with a SiO<sub>2</sub> tip. Optical properties were studied by UV-Vis-NIR spectroscopy, using a Jasco V-770 spectrophotometer in the range from 190 to 900 nm.

## III. RESULTS AND DISCUSSION

### III.1. Crystal structure.

X-Ray diffractograms of Al thin films synthesized under different RF power conditions are shown in Figure 1.

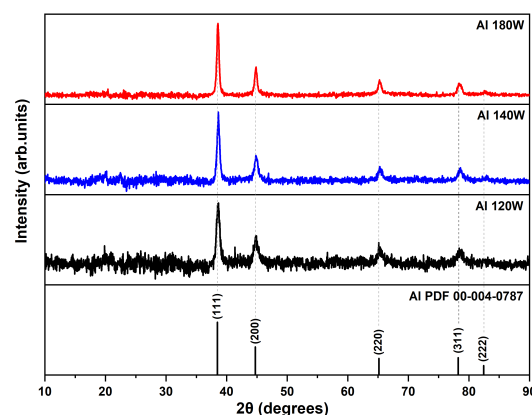


Figure 1. X-Ray diffractograms for the Al thin films obtained at different RF-power conditions.

The crystal structure of the obtained Al thin films corresponds to a face-centered cubic system with the space group Fm-3m (PDF 00-004-0787). The observed planes were (1 1 1), (2 0 0), (2 2 0), (3 1 1), and (2 2 2) for all thin films. A higher signal-to-noise (S/N) ratio was obtained with increasing RF power, attributed to the higher energy of the sputtered species depositing on the substrate's surface.

The crystallite size for the (111) diffraction plane was calculated using Scherrer's equation and Figure 2 shows its variation with RF power, increasing RF power resulted in a larger crystallite size. The higher crystal quality of the films is related to the deposition power since the sputtered species arrive with a higher kinetic energy, enhancing their surface mobility and allowing the adatoms to diffuse more easily across the surface. This enables them to reach energetically favorable lattice sites, promoting the formation of a well-ordered crystalline structure [19,20]. Moreover, at lower power, the critical nucleus size for film formation is smaller, leading to a higher nucleation density and the growth of finer grains, which can limit the overall crystallinity of the film [17].

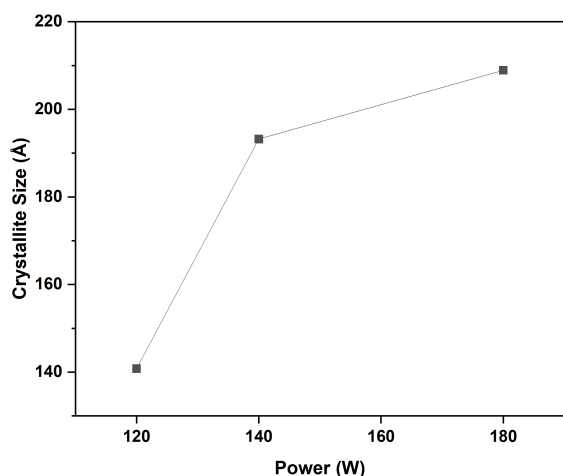


Figure 2. Crystallite size dependence on RF-power for the (111) diffraction plane in the Al thin films.

## III.2. Morphology.

### III.2.1. Scanning Electron Microscopy

The morphology of the deposited Al thin films was studied by field-emission scanning electron microscopy (FESEM). FESEM images are shown in Figure 3. The deposited Al thin films display features typical of magnetron-sputtered films, i.e., uniform dense films with high crystal quality [21, 22, 8] (see Figure 3 a-c). Figure 3(d-f) show the surface of the

thin films at higher magnifications. It can be appreciated that grain size increment as power increased. Histograms of the grain size with a fit to the log-normal distribution are shown in Figure 3 (g-i). The mean grain size of the Al thin films synthesized at 120, 140 and 180 W were 35 nm, 38, and 60 nm, respectively. The grain size dispersion was analyzed by means of the standard deviation of the fitted log-normal distribution. In this case, Al thin films deposited using 120, 140, and 180 W presented standard deviations of 13.0, 15.7, and 22.6 nm. The increase in grain size and its dispersion is related to the deposition power, which provides the sputtered species with energy to deposit on the glass substrate. At higher sputtering powers, the increased kinetic energy of aluminum atoms enhances their surface and grain boundary mobility, facilitating grain coalescence and growth [23, 24]. This increase in diffusion and grain coarsening lead to a gradual transition from small, island-like growth to thicker, columnar growth [17]. Furthermore, EDS spectra can be found in Figure 3 (j-l), where Al was detected in the surface of study. Elements such as O, Na, Mg, Si, and Ca were also detected in the spectra. These elements are present in the composition of the glass substrate.

Thin film thickness was measured using cross-section FESEM images. Figure 4(a-c) shows the thin films thickness for the Al thin films synthesized using 120, 140 and 180 W, respectively. Film thickness increased with RF power, from 170 nm for 120 W to 253 nm and 356 nm when using 140 and 180 W, respectively.

### III.2.2. Atomic Force Microscopy

Morphology of the deposited Al thin films was studied by Atomic Force Microscopy (AFM). Figure 5(a-c) shows the 3D and 2D micrographs for the films synthesized under different RF power conditions. As RF power increases, higher grain coalescence is observed. This resulted in denser films with larger grains and fewer grain boundaries. This observation agrees with the increment of crystallite size observed by XRD (see Section III.1).

Histograms of grain size, with a fit to the log-normal distribution, are shown in Figure 6. The mean grain sizes of the Al thin films were 30 nm, 36 nm, and 54 nm, with standard deviations of 10.1 nm, 16.1 nm, and 22.1 nm, for the synthesis powers of 120 W, 140 W, and 180 W, respectively.

Figure 7 exhibits the evolution of thin films' thickness and RMS roughness. Higher thickness and RMS roughness were obtained at higher RF power. When RF power increased from 120 to 180 W, thickness of the Al thin films increased from 163 to 328 nm, while RMS roughness changed from 4.50 to 17.09 nm. Table 2 summarizes the obtained thickness, deposition rate and RMS roughness for each deposition condition employed.



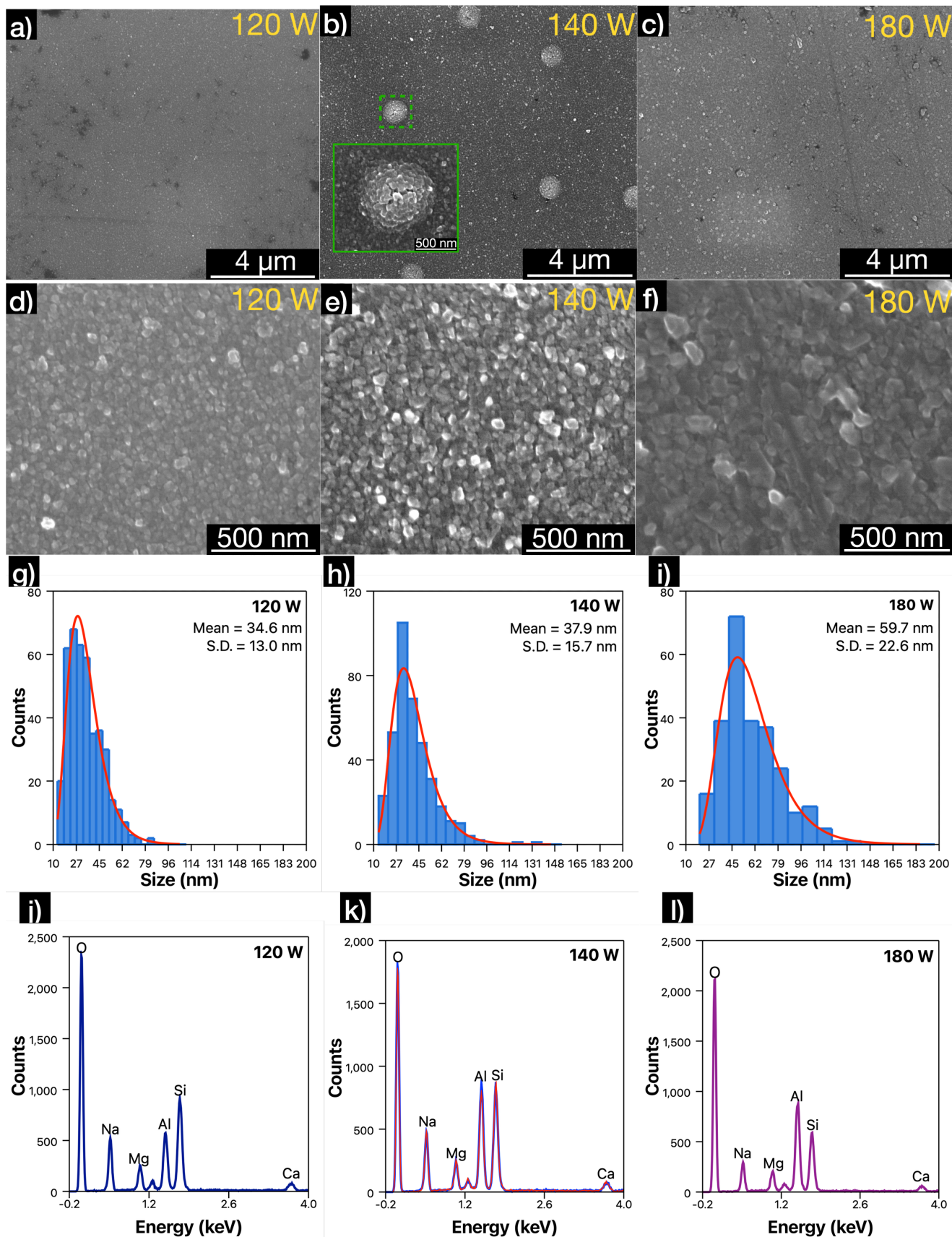


Figure 3. (a-f) FESEM images for Al thin films synthesized at 120, 140, and 180 W at different magnifications. (g-i) Grain size distribution of Al thin films synthesized using 120, 140 and 180 W. (j-l) EDS spectra of the Al thin films synthesized at 120, 140, and 180 W.



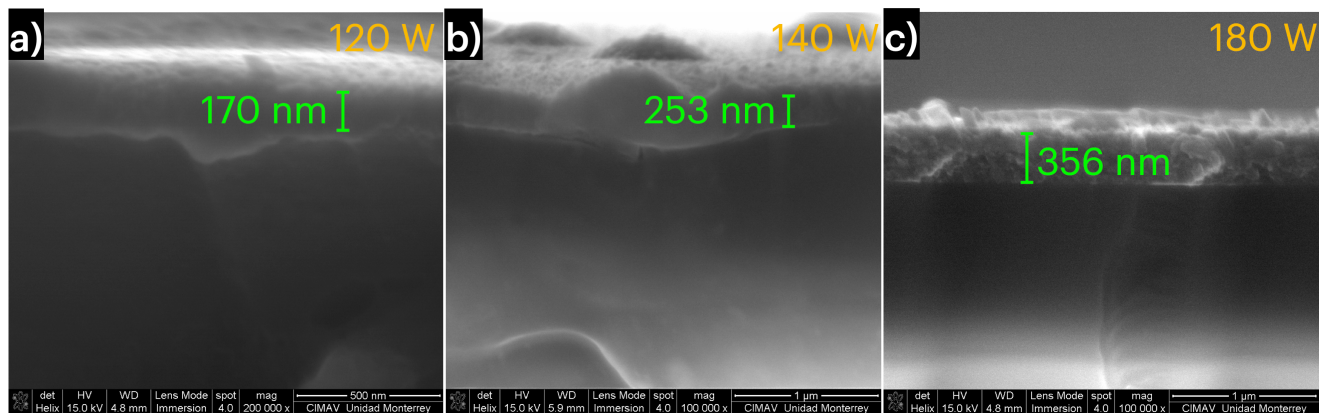


Figure 4. (a-c) Cross-sectional FESEM images for Al thin films synthesized at 120, 140, and 180 W, respectively.

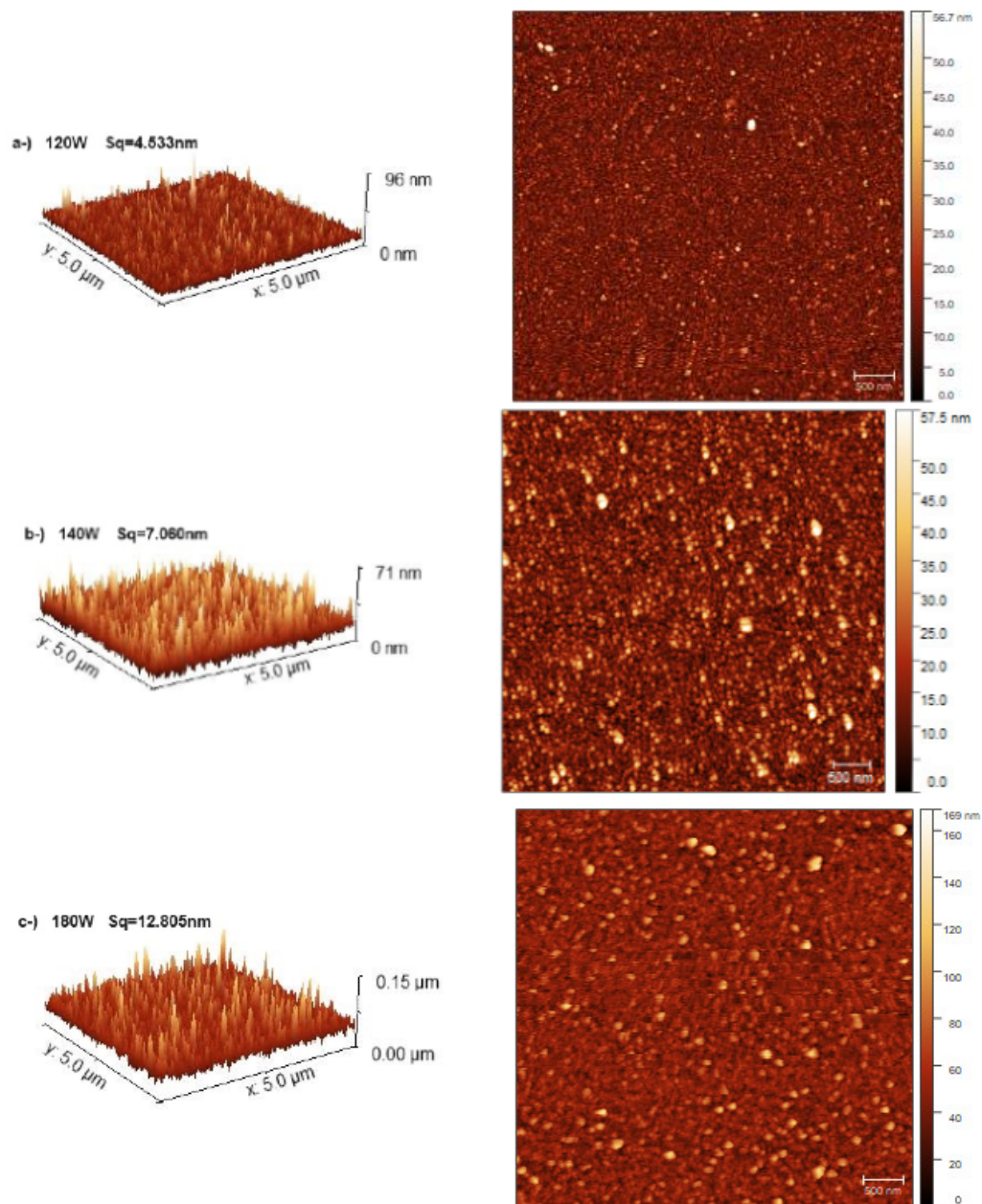


Figure 5. AFM images for the Al thin films synthesized at a) 120, b) 140 and c) 180 W.

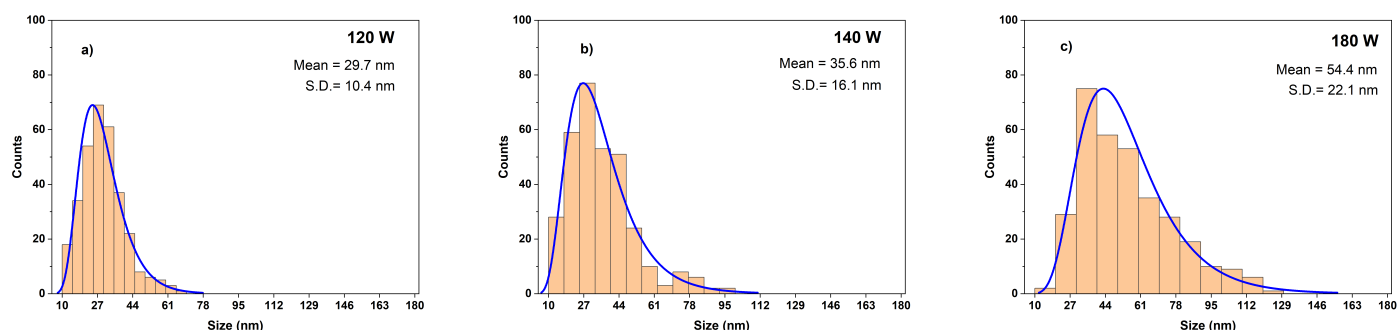


Figure 6. Grain size distribution of Al thin films synthesized using 120, 140 and 180 W.

At high RF power, argon gas and sputtered particles gain significant kinetic energy, which may lead to: (i) an increased deposition rate, and (ii) more frequent collisions between target atoms and ions, reducing the mean-free-path of the target atoms and therefore lowering film growth [20]. In our study, higher power led to increased deposition rates and the formation of thicker aluminum films.

Table 2. Morphological properties of the Al thin films synthesized under different RF power conditions.

Property	Power (W)		
	120	140	180
Thickness (nm)	163	218	328
Deposition rate (nm/min)	10.87	14.53	21.87
RMS roughness (nm)	4.53	7.06	12.80

Table 3 summarizes the results for mean grain size and film thickness obtained through Scanning Electron Microscopy and Atomic Force Microscopy. Grain sizes measured by AFM tend to be slightly smaller than those from SEM. This difference may arise from the AFM's higher surface sensitivity and resolution, which allow it to resolve finer grain boundaries more precisely [25].

Table 3. Comparison of grain size and film thickness measured by SEM and AFM

Property	120 W	140 W	180 W
Mean Grain Size (nm) - SEM	35	38	60
Film Thickness (nm) - SEM	170	253	356
Mean Grain Size (nm) - AFM	30	36	54
Film Thickness (nm) - AFM	163	218	328

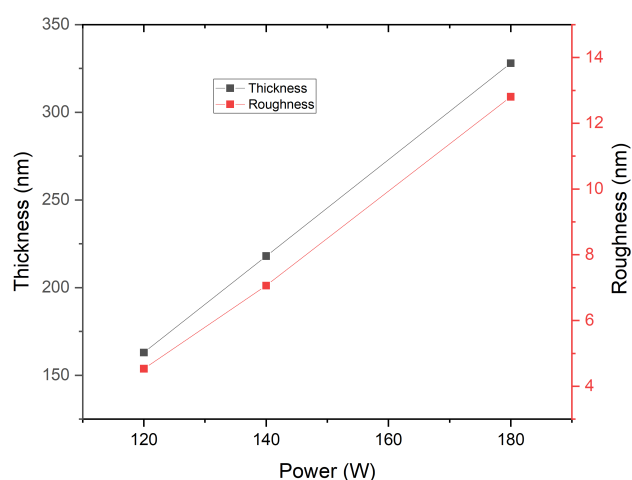


Figure 7. Thickness and RMS roughness development against RF power.

### III.3. Optical properties.

Optical properties of the Al thin films were assessed by UV-Vis-NIR spectroscopy. Diffuse reflectance of the samples is shown in Figure 8. Films presented high diffuse reflectance (above 60%) in the visible range of the electromagnetic spectrum (380-750 nm). It is well known that structural and morphological properties have a direct impact on the optical properties of thin films [23, 1]. Higher sputtering power led to increased thickness, larger crystallite sizes, and higher surface roughness, which enhances light scattering. This results in a higher diffuse reflectance signal [26, 27].

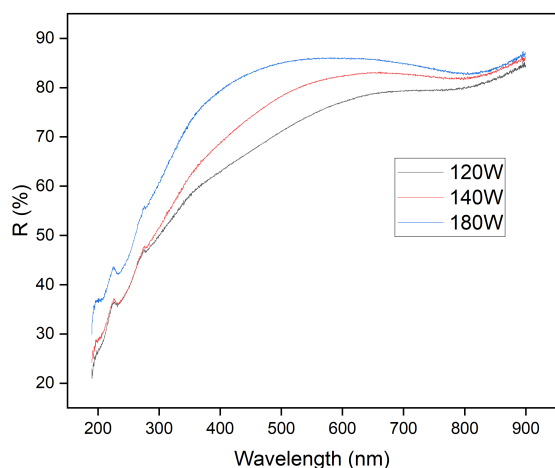


Figure 8. Diffuse reflectance of the Al thin films synthesized under different power conditions.

#### IV. CONCLUSION

Al thin films have been synthesized by RF magnetron sputtering on BK7 glass substrates. The effect of RF power on their structural, morphological, and optical properties was investigated. Deposition using higher RF power resulted in improved structural and morphological properties, i.e., denser Al thin films with higher crystal quality (larger crystallite size) as well as greater grain size were obtained. The improvement of the structural and morphological properties led to enhanced diffuse reflectance. The RF power used during deposition is related to the kinetic energy of the sputtered species; thus, higher power during deposition enhances their mobility on the surface and through grain boundaries, facilitating the grain coalescence and growth.

#### V. ACKNOWLEDGEMENT

We acknowledge Dr. Maria Isabel Mendivil Palma from CIMAV Monterrey for her help measuring SEM images and EDS spectra. R. Ramos Blazquez acknowledges CONAHCYT for his master studies scholarship (843048).

A. Collado-Hernandez thanks CONAHCYT for his doctoral studies scholarship (841625). We thank an anonymous referee for valuable critique and suggestions.

#### REFERENCES

- [1] F. M. Mwema, O. P. Oladimeji, S. A. Akinlabi, and E. T. Akinlabi, *J. Alloys Compd.* **747**, 306 (2018).
- [2] B. Wu *et al.*, *Vacuum* **150**, 144 (2018).
- [3] A. Iqbal and F. Mohd-Yasin, *Sensors* **18**, 1797 (2018).
- [4] M. D. Serna-Manrique *et al.*, *Coatings* **12**(7), 979 (2022).
- [5] R. S. Tondare *et al.*, *Mater. Today Proc.* **5**, 2710 (2018).
- [6] A. Tchenka *et al.*, *Adv. Mat. Sci. Eng.* **2021**, 5556305 (2021).
- [7] J. Wang *et al.*, *Appl. Surf. Sci.* **515**, 146053 (2020).
- [8] M. K. Sandager, C. Kjelde, and V. Popok, *Crystals* **12**, 1379 (2022).
- [9] Y. Gao, H. Leiste, S. Heissler, S. Ulrich, and M. Stueber, *Thin Solid Films* **660**, 439 (2018).
- [10] S. Ponmudi, R. Sivakumar, C. Sanjeeviraja, and C. Gopalakrishnan, *J. Mater. Sci.: Mater. Electron.* **30**, 18315 (2019).
- [11] C. Liu, J. Peng, Z. Xu, Q. Shen, and C. Wang, *Metals* **13**, 583 (2023).
- [12] H. A. R. O. O. N. Ejaz *et al.*, *J. Appl. Chem. Sci. Int.* **13**, 41 (2022).
- [13] M. Singh *et al.*, *Mater. Today Proc.* **5**, 2696 (2018).
- [14] F. Madaraka *et al.*, *Mater. Today Proc.* **5**, 20464 (2018).
- [15] K. Balasubramanian *et al.*, *Proc. SPIE* **9602**, 96020I (2015).
- [16] S. Pogodin *et al.*, *Biophys. J.* **104**, 835 (2013).
- [17] C. Zhou, T. Li, X. Wei, and B. Yan, *Metals* **10**, 896 (2020).
- [18] A. Iqbal *et al.*, *J. Mater. Sci.: Mater. Electron.* **31**(1), 239 (2020).
- [19] S. Yu, W. Xu, H. Zhu *et al.*, *J. Alloys Compd.* **883**, 160622 (2021).
- [20] S. Asgary *et al.*, *Appl. Phys. A* **127**, 752 (2021).
- [21] J. Li, G. K. Ren, J. Chen *et al.*, *JOM* **74**, 3069 (2022).
- [22] J. Cheng *et al.*, *Chem. Eng. J.* **509**, 161242 (2025).
- [23] D. Zöllner, *Comput. Mater. Sci.* **125**, 51 (2016).
- [24] V. Karoutsos *et al.*, *Coatings* **14**, 1441 (2024).
- [25] L. Crouzier *et al.*, *Beilstein J. Nanotechnol.* **10**, 1523 (2019).
- [26] G. Rincón-Llorente *et al.*, *Coatings* **8**, 321 (2018).
- [27] C. A. Corrêa *et al.*, *RSC Adv.* **14**, 15220 (2024).

This work is licensed under the Creative Commons Attribution-NonCommercial 4.0 International (CC BY-NC 4.0, <https://creativecommons.org/licenses/by-nc/4.0/>) license.

